

ELMs and the H-mode pedestal in NSTX

R. Maingi ^{a,*}, S.A. Sabbagh ^b, C.E. Bush ^a, E.D. Fredrickson ^c,
J.E. Menard ^c, D. Stutman ^d, K. Tritz ^d, M.G. Bell ^c,
R.E. Bell ^c, J.A. Boedo ^e, D.A. Gates ^c, D.W. Johnson ^c, R. Kaita ^c,
S.M. Kaye ^c, H.W. Kugel ^c, B.P. LeBlanc ^c, D. Mueller ^c, R. Raman ^f,
A.L. Roquemore ^c, V.A. Soukhanovskii ^g, T. Stevenson ^c

^a Oak Ridge National Laboratory, P.O. Box 2009, Oak Ridge, TN 37831-8072, USA

^b Columbia University, New York, NY 10027, USA

^c Princeton Plasma Physics Laboratory, P.O. Box 451, Princeton, NJ 08543, USA

^d Johns Hopkins University, Baltimore, MD 20723-6099, USA

^e University of California San Diego, San Diego CA 92093-0319, USA

^f University of Washington, Seattle WA 98195-4290, USA

^g Lawrence Livermore National Lab, Livermore CA 94550, USA

Abstract

We report on the behavior of ELMs in NBI-heated H-mode plasmas in NSTX. It is observed that the size of Type I ELMs, characterized by the change in plasma energy, decreases with increasing line-average density, as observed at conventional aspect ratio. It is also observed that the Type I ELM size decreases as the plasma equilibrium is shifted from a symmetric double-null toward a lower single-null configuration. Type II/III ELMs have also been observed in NSTX, as well as a high-performance regime with small ELMs which we designate Type V. The Type V ELMs are characterized by an intermittent $n = 1$ magnetic pre-cursor oscillation rotating counter to the plasma current; the mode vanishes between Type V ELMs crashes. Without active pumping, the density rises continuously through the Type V phase, albeit at a slower rate than ELM-free discharges.

© 2004 Elsevier B.V. All rights reserved.

PACS: 52.55.Fa; 52.55.Rk

Keywords: ELM; Edge pedestal; Fueling; NSTX; Particle control

1. Introduction

Edge localized modes (ELMs) have been observed in tokamaks since the discovery of the H-mode. ELMs prevent build-up of fuel and impurity particles by periodic ejection of the edge plasma into the scrape-off layer and divertor plasma, where they may be exhausted. This periodic ejection results in transiently high power and

* Corresponding author. Address: Princeton Plasma Physics Lab, Receiving 3, Route 1 North, Princeton, NJ 08543, USA. Tel.: +1 609 243 3176; fax: +1 609 243 3233.

E-mail address: rmaingi@pppl.gov (R. Maingi).

particle loads to the plasma facing components (PFC). Nonetheless, the baseline operating scenario for the International Thermonuclear Experimental Reactor (ITER) relies on H-Mode confinement and profiles [1], partly because the best plasma performance is often realized in the so-called Type I ELM regime. The Type I ELM typically results in larger heat pulses than other ELM types [2]. Such transient PFC loading is tolerable in present day machines, but extrapolations show that severe PFC damage may occur in larger, higher power density machines (such as ITER) when the ELM power loading exceeds material limits. Thus the scaling of power loss to PFCs during Type I ELMs, as well as the search for smaller/no ELM regimes with good performance, has received significant attention in fusion research.

A wide variety of ELMs has been observed in the National Spherical Torus Experiment (NSTX), including Type I, Type II/III, and a new small ELM regime which we label as ‘Type V’. Type I ELMs are observed in intermediate neutral beam injection (NBI) power double-null discharges and high NBI power lower single null discharges. Type II/III ELMs are observed at high elongation $\kappa \geq 2$ and with heating power close to and well above the L-H power threshold, but at the moment, only in shapes close to double-null (hence the ambiguity in identification). Type V ELMs are observed over a wide heating power range in lower single-nulls. In brief, Type V ELMs have a distinct electromagnetic pre-cursor and do not require either a shape change or high poloidal beta as needed for Type II or ‘grassy’ ELMs (note that Type IV ELM classification was used briefly in the mid-1990’s by the DIII-D team during pumping experiments). The pedestal collisionality in all NSTX ELM regimes is relatively high with $\nu^* \geq 0.5$. In the remainder of this section and the next, the ELM observations and the results of an experiment to study Type I ELM scaling will be described. Type V ELM characteristics will be described in Section 3, and other details are presented elsewhere [3].

The NSTX is a medium-sized, low-aspect ratio spherical tokamak [4] with the following parameters: major radius $R = 0.85\text{m}$, minor radius $a = 0.67\text{m}$, $R/a \geq 1.26$, toroidal field $B_t \leq 0.6\text{T}$, with up to 7MW of NBI power (P_{NBI}) and 6MW of radio-frequency heating. Fig. 1 shows a survey of ELM types in NSTX, along with the corresponding impact on the plasma stored energy. Panel (a) shows Type I ELMs, which reduce the plasma stored energy by up to 10%. Panel (b) shows Type II/III ELMs, which decrease the stored energy by 1–3%. The Type II/III ELMs are identified by their inverse heating power/frequency relationship, their occurrence close to the L–H power threshold, and the presence of a long-lived electromagnetic pre-cursor oscillation. Panel (c) shows a regime characterized by tiny, rapid ELMs which we designate as Type V [5]; each ELM has an indiscernible

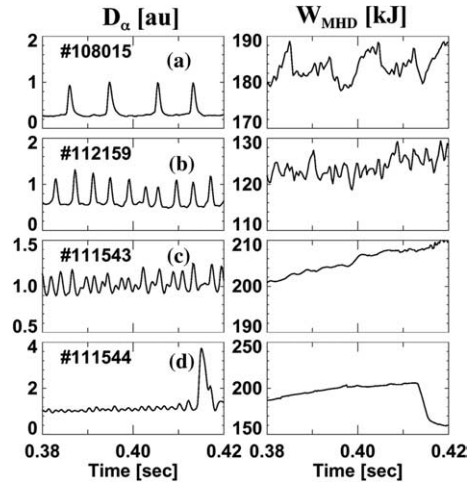


Fig. 1. Different ELM types observed in NSTX: (a) Type I, (b) Type II/III, (c) new, Type V, and (d) mixed Type V with a ‘giant’ ELM.

impact on stored energy, although the particle and energy confinement in this Type V ELM regime are reduced compared with ELM-free discharges. Panel (d) shows a mixed ELM regime with Type V ELMs and a giant event, which can reduce the stored energy by 30%. The giant events are sometimes seen under low recycling conditions (e.g. see the next Section 2) and are independent from the Type V ELMs.

2. ELM size and frequency scaling experiments

The Type I ELM size and frequency scaling experiments were conducted in diverted discharges with $I_p = 0.9\text{MA}$, $B_t = 0.45\text{T}$, $\kappa \sim 1.9$, with the ion grad-B drift toward the lower X-point. At the time of these experiments, high triangularity ($\delta \sim 0.8$) double-null discharges were studied because Type I ELMs were readily obtained [6]. The size of the ELM was computed from fast EFIT reconstructions [7,8] with 0.25ms resolution. Here ELM size is measured by the change in stored energy (ΔW) due to the ELM, relative to both the initial stored energy W_0 and the pedestal stored energy W_{ped} . The pedestal pressure was obtained by fitting the electron pressure profile with a (‘standard’) modified hyperbolic tangent. The pedestal stored energy was obtained by $W_{\text{ped}} = 0.92 * 3 * P_{e,\text{ped}} * V_{\text{pl}}$, as used for multi-machine scalings [9]. Here $P_{e,\text{ped}}$ is the fitted electron pedestal pressure and V_{pl} is the plasma volume. Typically the pedestal stored energy fraction W_{ped}/W_0 lies between 25% and 33%. We also note that the pedestal stored energy computed with the above equation for NSTX usually lies within 20% of the value predicted by the recent multi-machine scaling [9].

In principle, this technique allows resolution of ELMs up to ~ 1 kHz frequency, but practically the size becomes limited both by statistics ($\pm 1-1.5\%$) and by the eddy current model used in the present reconstructions, the latter becoming more unreliable as the speed of the transients increases. Thus the ELM size scaling for frequencies above 300 Hz should be viewed only as an indication of the trend.

One feature prevalent in most NSTX H-mode discharges with NBI heating is a secular density ramp, due partly to good particle confinement time and partly to continuous fueling by both the neutral beams themselves and by gas injected from the center stack midplane. This center-stack fueling was found to facilitate reproducible H-mode access [10,11], but the limited space there prevents installation of a fast time response control valve. Hence the center stack gas injector has a 0.55 s e-folding decay time for the flow rate. Fig. 2 shows the discharge characteristics for a fueling rate scan obtained by using different fill pressures on the center stack midplane injector in a double-null discharge. It is observed that the density rate of rise increased modestly with the flow rate. At the lowest flow rate, a clear H-mode transition could not be obtained, although there were sometimes dithering transitions in and out of H-mode. It can also be seen that the D_α modulations due to the ELMs decreased with increasing density. Fig. 3(a–c) shows the results of the ELM size analysis for all Type I ELMs in the fueling rate scan from $\sim t = 0.27 - 0.34$ s, which corresponds to the time of constant NBI power ~ 3.7 MW. Note that the ELM size actually shrunk once the NBI power was dropped after ~ 0.34 s in these discharges (except for #108470, when the NBI power was reduced at 0.3 s). There is a large

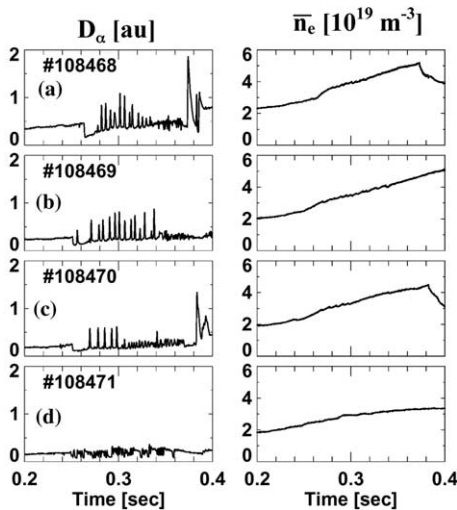


Fig. 2. Flow rate scan in double-null configuration: (a) 39 Torr-l/s average flow, (b) 14 Torr-l/s, (c) 9 Torr-l/s, and (d) 3 Torr-l/s.

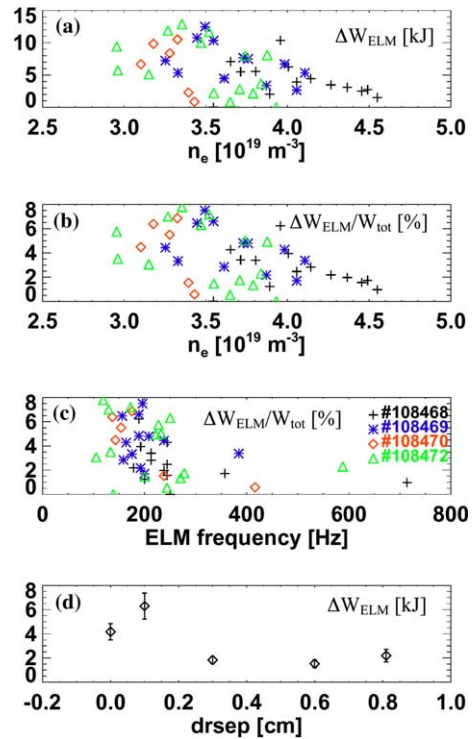


Fig. 3. Type I ELM size scaling: (a) ELM loss size vs. \bar{n}_e , (b) ELM energy loss fraction vs. \bar{n}_e , (c) ELM energy loss fraction vs. frequency, and (d) ELM loss size vs. $drsep$ (see text).

variation in the ELM size, but the envelope appears to shrink with increasing density, as observed at conventional aspect ratio [12]. This observation of a dependence of ELM size on line-average density was confirmed in subsequent experiments with constant NBI power over a larger density range. The maximum stored energy loss fraction $\Delta W/W_0$ in this scan approached 8%, and the pedestal loss fraction $\Delta W/W_{ped}$ approached 30%. The frequency of the ELMs generally increased with density. Fig. 3(c) shows that the ELM size generally decreased as the frequency increased. We note that the average ELM size at each fueling rate did not scale with the fueling rate itself, i.e. the density dependence was the primary factor affecting ELM size and frequency.

Fig. 3(d) shows the average ELM size observed during a divertor configuration scan. Here the change in configuration was characterized by the parameter $drsep$, defined as the distance at the outer midplane between the separatrix flux surfaces passing through the upper and lower X-points, with the convention that a positive $drsep$ favors the lower divertor. Although the scan is sparse, it does appear that the average ELM size is reduced somewhere between a balanced double-null ($drsep = 0$) and a ‘true’ lower single-null, e.g. with $drsep >$

the ion poloidal gyro-radius (~ 1 cm for these conditions). While these preliminary results require confirmation with a finer *drsep* scan, it is notable that similar results were reported on ASDEX-Upgrade, along with the assertion [13] that the ELM type became grassy or Type II. We also note that *drsep* parameter plays a role in determining the L–H power threshold [14].

Finally a power scan showed no clear effect on ELM size. The discharges became ELM-free as heating power approached the L–H transition power. In these cases, sawteeth were observed which dropped the stored energy by up to 20%, but individual ELMs were not present.

Single-null discharges exhibit the same secular density rise present in double-nulls, and as with the double-nulls, a minimum fueling rate is required to access H-mode. However routine Type I ELM activity is uncommon in NSTX single-null discharges. At medium and high fueling rates, rapid Type V ELMs were observed. As the fueling rate was reduced to just above the minimum required for H-mode access, giant ELMs (with $\Delta W/W_0$ up to 30%) were observed. The physics of these large events is not well understood; stability calculations suggest the high-*n* ballooning mode as a candidate [6]. For the Type V ELMs, a scan of the inner wall gap showed that the characteristics did not markedly change until the plasma was re-limited on the center stack, at which point an H–L transition was observed.

3. Type V ELM characteristics

The basic characteristics of the NSTX high performance, Type V ELM regime were shown in Fig. 1 of Ref. [5] for a lower-single null diverted discharge with $I_p = 0.8$ MA, $B_t = 0.5$ T, $P_{\text{NBI}} = 4.1$ MW, elongation $\kappa \sim 1.9$, lower triangularity $\delta_L \sim 0.5$, and upper triangularity $\delta_U \sim 0.3$. The line density continuously rose after the H-mode transition at $t = 230$ ms. Type V ELMs with a frequency ~ 400 Hz were observed on the lower divertor D_α starting at $t \sim 340$ ms, although a few irregularly spaced Type V ELMs were observed near 290 and 320 ms. Gas puffing from the center stack continued throughout the discharge; the combination of this and the NBI fueling contributed to the observed density rise. The stored energy remained flat for about 370 ms or $\sim 7^* \tau_E$, and the confinement enhancement over ITER-89P scaling [15] was steady at ~ 2.3 .

As mentioned previously, the Type V ELMs have no individual measurable impact on stored energy, but they are observed both in the radial profile of divertor D_α emission, the ultra-soft X-ray (USXR) diagnostic [16], and a fast reciprocating probe introduced into the edge plasma. The ELMs increase the entire divertor D_α profile by ~ 20 – 30% , similar to the impact observed in the spatially integrated channels.

These ELMs are not the result of a persistent, i.e. continuous MHD mode. Low-*n* intermediate frequency (20–80 kHz) coherent modes were observed in the core from 300–700 ms, but these modes started shortly after the Type V ELM activity. In other discharges it was observed that these coherent modes persisted even after the Type V ELMs stopped. Thus it is probable that these coherent modes are not the source of the ELMs, but rather a by-product of the conditions set-up in this high performance regime.

Nonetheless, the Type V ELMs have a distinct electromagnetic pre-cursor. An $n = 1$ mode is observed in a toroidal Mirnov array below the outer midplane (Fig. 4) a few hundred microseconds before the USXR perturbation. The mode propagates in the counter plasma current direction and persists for ~ 2 toroidal transit times before dissipating (and re-appearing before the next ELM crash). The poloidal propagation of the mode is observed on a poloidal Mirnov array in the NSTX passive stabilizing plates and in the USXR system. The mode is first observed typically in the lower divertor and propagates to the outer midplane and then the top of the machine. The propagation down the inboard side of the machine is not observable due to diagnostic limitations, but the example in Fig. 4 re-appears in the lower

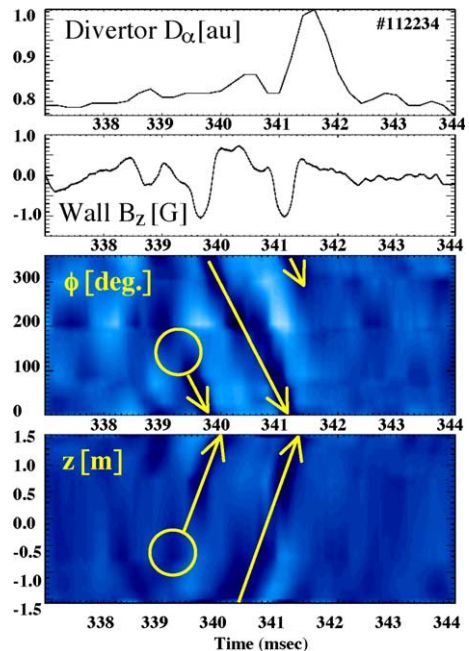


Fig. 4. Magnetic pre-cursor of Type V ELM crashes: (a) divertor D_α , (b) magnetic perturbation size at wall at $\phi = 30^\circ$, (c) toroidal Mirnov array with dark blue bands showing mode toroidal propagation counter to I_p , and (d) passive plate Mirnov array with dark blue bands showing mode poloidal propagation upward. The approximate mode birth is highlighted by circles in (c) and (d).

divertor region and propagates upward again. The last temporal signature is the divertor D_α rise, which occurs a few hundred microseconds afterwards. The characteristics of these ELMs have some similarities to observations of SOL current reported from conventional aspect ratio tokamaks [17].

4. Summary, discussion and conclusions

Many different ELM types have been observed in NSTX, including conventional Type I, Type II/III, a new small ELM (which we designate as Type V), and ‘giant’ ELMs. The Type I ELMs reduce the plasma stored energy by up to 10%, and the pedestal energy by up to 30%. The size of these Type I ELMs decreases with density and as the magnetic configuration is shifted from a double-null to a lower-single null. Giant ELMs (which may just be Type I ELMs with a large crash, but are clearly not ‘compound’ ELMs with a prolonged L-mode phase) are observed under low recycling conditions in lower-single null configuration and can decrease the plasma stored energy by up to 30%. The Type V ELM regime is observed in high density, high performance discharges. The Type V ELMs have a short-lived $n = 1$ pre-cursor mode rotating counter to the plasma current, and are observed in a poloidal Mirnov array and the USXR, as well as the divertor D_α profile.

The NSTX Type V regime appears to be distinct from the DIII-D quiescent H-mode, which requires an edge harmonic oscillation for particle control. The NSTX Type V regime is also distinct from the PDX forced density rise scenario and the Alcator C-MOD Enhanced D_α H-mode, which require an edge quasi-coherent mode for particle control. Experiments to determine the underlying physical mechanisms for Type V ELMs, as well as to test the extrapolability to low collisionality conventional aspect ratio tokamaks and to assess the level of particle control provided by these ELMs, are being considered.

Acknowledgments

This research was supported by the US Dept. of Energy under contracts DE-AC05-00OR22725, DE-AC02-76CH03073, and W-7405-ENG-36, and grants DE-FG03-95ER54294, DE-FG02-99ER54519, DE-FG02-99ER54523, and DE-FG02-99ER54524. We gratefully acknowledge the contributions of the NSTX operations staff.

References

- [1] I.P.B. Authors et al., Nucl. Fus. 39 (1999) 2137.
- [2] A. Loarte et al., J. Nucl. Mater. 313–316 (2003) 962.
- [3] R. Maingi et al., Proceedings of the 31st EPS Conference on Plasma Physics and Contr. Fusion, London, UK, 28 June–2 July 2004 28G (2004) Paper P2.189.
- [4] M. Ono et al., Nucl. Fus. 40 (2000) 557.
- [5] R. Maingi et al., Observation of a High Performance Operating Regime with Small Edge-Localized Modes in the National Spherical Torus Experiment. Nucl. Fus., submitted for publication.
- [6] C.E. Bush et al., Phys. Plasmas 10 (2003) 1755.
- [7] L.L. Lao et al., Nucl. Fus. 25 (1985) 1611.
- [8] S.A. Sabbagh et al., Nucl. Fus. 41 (2001) 1601.
- [9] J.G. Cordey et al., Nucl. Fus. 43 (2003) 670.
- [10] R. Maingi et al., Nucl. Fus. 43 (2003) 969.
- [11] R. Maingi et al., Plasma Phys. Control. Fus. 46 (2004) A305.
- [12] A.W. Leonard et al., J. Nucl. Mater. 290–293 (2001) 1097.
- [13] O. Gruber et al., Proceedings of the 19th International Conference on Plasma Physics and Controlled Fusion, Lyon, 2002 (IAEA, Vienna) (2002) paper EX/C2.
- [14] H. Meyer et al., Plasma Phys. Control. Fus. 46 (2004) A291.
- [15] P.N. Yushmanov et al., Nucl. Fus. 30 (1990) 1999.
- [16] D. Stutman et al., Rev. Sci. Instrum. 74 (2003) 1982.
- [17] H. Takahashi et al., Nucl. Fus. 44 (2004) 1075.